Chemical Science Review and Letters ISSN 2278-6783

www.chesci.com Research Article

# Synthesis, Spectral Characterization, DNA Cleavage, and Antimicrobial Activity of Transition Metal (II) Complexes of Pyranochromene Derivatives

Disha Tilala[1]*, Kamlesh Gurjar[1], Naveen Kumar Sharma[2] and Denish Karia[3]

[1]Vishwakarma government engineering college, Chandkheda, Ahmedabad- 382424 (Gujarat) India
[2]L.E. College, Morbi- 363642 (Gujarat) India
[3]Department of Chemistry, Patel J. D. K. Davolwala Science College, Borsad-388540 (Gujarat) India

**Abstract**

New ligands $L^{III}$ = 3-acetyl-4-hydroxy-7-methylpyrano [3,2-*c*]chromene-2,5-dione, $L^{IX}$ = 4-hydroxy-7-methyl-3-(3-oxobutanoyl)pyrano[3,2-c]chromene-2,5-dione and their metal(II) complexes $M[L^{III}(H_2O)]_2$ and $M[L^{IX}(H_2O)]_2$ were synthesized using transition metals iron, cobalt, nickel and characterized by UV, FT-IR, mass spectra, 1H NMR and elemental analysis,. The conductivity of metal complexes was determined. In the presence of $H_2O_2$ at 37°C, complexes can efficiently cleave Calf Thymus DNA. Ligands and their metal (II) complexes also show good *in vitro* antimicrobial activity. Copper complexes of both ligands have highest DNA cleavage ability and also shows maximum zone of inhibition indicating higher antimicrobial activities.

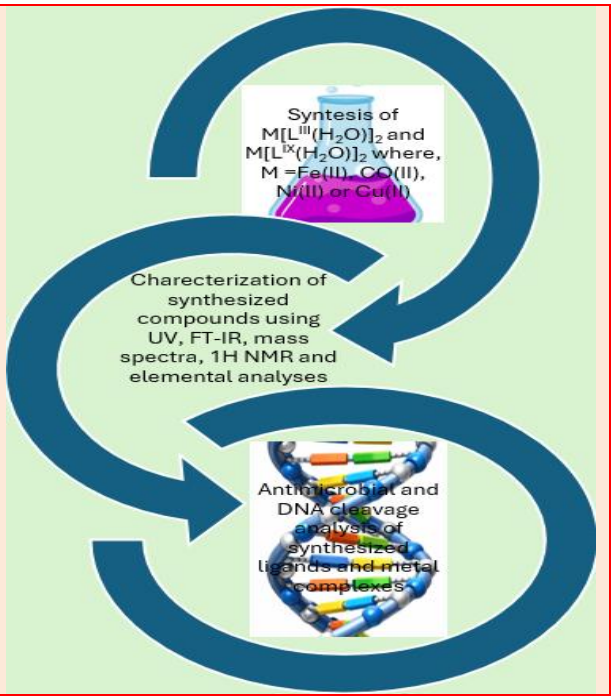


**Keywords:** metal (II) complexes, Calf Thymus DNA, antimicrobial, *in vitro*

***Correspondence**
Author: Disha Tilala

## Introduction

The search for innovative molecular combinations to develop novel antimicrobial and antiviral agents has attracted substantial global attention in recent years [1, 2], primarily due to the escalating concern over the rapid emergence of antibiotic-resistant bacteria. This alarming trend is further intensified by the significant lack of newly developed antibiotic classes, resulting in what is widely referred to as an “antibacterial crisis” [3]. Similarly, fungal infections are emerging as a major cause of morbidity and mortality, particularly among immunocompromised individuals. The increasing prevalence of mycoses is largely attributed to the progressive development of resistance to antifungal agents used in clinical practice, along with the limited diversity of available antifungal drug classes, which significantly restricts therapeutic options [4].

In biological systems, metal ions such as zinc and copper play indispensable roles in maintaining normal physiological functions [5]. Transition metals including copper, iron, and manganese participate in a wide range of biochemical processes, encompassing electron transfer, enzymatic catalysis, and structural stabilization. These metals are commonly localized at the active sites of proteins and enzymes, where they facilitate essential cellular reactions [5]. Despite their vital importance, deregulations of these essential metals during normal biochemical processes has been associated with the onset and progression of various pathological conditions, including cancer [6]. Cellular functions require these “trace metals” only in minute but strictly regulated concentrations, as both deficiency and excess can disrupt cellular functions. In recent years, substantial progress has been achieved in exploiting transition metal complexes for therapeutic applications in the treatment of several human diseases. The ability of transition metals to adopt multiple oxidation states and to coordinate with negatively charged biomolecules underlies their diverse reactivity

and biological activity. These distinctive chemical properties have fostered the development of metal-based drugs with promising pharmacological potential and unique therapeutic advantages over purely organic compounds [5].

In the present study, the synthesis and characterization of the ligand and its corresponding metal complexes were accomplished using various spectroscopic techniques. The antimicrobial activity of the synthesized compounds was evaluated against bacterial strains *E. coli* and *B. megaterium*, while antifungal activity was assessed against *C. albicans* and *A. niger*. Furthermore, the nuclease activity of the complexes toward calf thymus (CT) DNA was investigated using the gel electrophoresis technique.

## Experimental

### *Apparatus and reagents*

All chemicals used in this study were of analytical reagent (AR) grade and of the highest purity available. The reagents included phenol, zinc chloride, sodium carbonate, ammonia, malonic acid, phosphorus oxychloride (Spectrochem), ethanol, hydrochloric acid, glucose, nutrient broth, agarose (Merck), and yeast extract (Helini Biomolecules). Calf thymus DNA (CT-DNA) was procured from Genei Chemical Company, India. CT-DNA solutions were prepared in Tris–HCl/NaCl buffer (pH 7.2) and showed an A260/A280 ratio of approximately 1.8–1.9, confirming the absence of significant protein contamination [7]. Double-distilled water was used to prepare all buffer solutions. Stock solutions were stored at 4 °C and used within four days.

Melting points were determined in open glass capillaries using a liquid paraffin bath and are uncorrected. The molar conductance of the metal complexes was measured using a Systronics conductivity bridge. UV–Vis spectra were recorded on a Shimadzu UV-1800 spectrophotometer (Shimadzu Pvt. Ltd., Japan). IR spectra were measured on a Shimadzu 435-IR spectrophotometer in the frequency range 4000–400 $cm^{-1}$ using the KBr pellet technique. Mass spectra were obtained on a GCMS-QP2010 spectrometer using the electron ionization (EI) method. 1H NMR spectra were recorded on a Bruker NMR spectrometer operating at 300 MHz.

### *Synthesis of 4-hydroxy-7-methyl-2H-chromene-2-one (1)*

The ligand was synthesized according to the reported procedure of Shah et al. [8] with slight modification. o-Cresol (0.1 mol) and malonic acid (0.1 mol) were added slowly to a mixture of phosphorus oxychloride (40 mL) and freshly fused zinc chloride (40 g) under constant stirring. The reaction mixture was heated on a water bath at 60–70 °C for 8–12 h. After completion of the reaction (monitored by TLC using solvent system ethyl acetate and hexane ratio 6:4), the mixture was poured onto crushed ice with continuous stirring. The resulting solid was filtered and treated with hot saturated sodium carbonate solution. The filtrate obtained was gradually acidified with concentrated hydrochloric acid until neutralization, leading to the formation of a precipitate. The solid product was collected by filtration, washed thoroughly with water, dried and recrystallized from methanol to afford the pure compound. The yield is found out to be about 78%.

### *Synthesis of 4-hydroxy-7-methylpyrano[3,2-c]chromene-2,5-dione (2)*

A mixture of phosphorous oxychloride (40ml) and freshly fused zinc chloride (40g) was prepared and malonic acid (0.1mole). 4-hydroxy-7-methyl-2*H*-chromene-2-one (0.1mole) were added to this mixture and heated on water bath at 60-70°C for 18-22 h. After completion of the reaction, the mixture was poured onto crushed ice with continuous stirring. The resulting solid was filtered and treated with hot saturated sodium carbonate solution. The filtrate obtained was gradually acidified with concentrated hydrochloric acid until neutralization, resulting in the formation of a precipitate. The solid product was collected by filtration, washed thoroughly with water, dried, and recrystallized from methanol to afford the pure. The yield is found out to be about 73%.

### *Synthesis of 3-acetyl-4-hydroxy-7-methyl-pyrano[3,2-c]chromene-2,5-dione ($L^{III}$)*

Acetyl derivatives were prepared by acetylation of different derivatives in presence of acetic acid and phosphorous oxychloride [9-14]. Glacial acetic acid (5ml) and phosphorous oxychloride (4ml) were used to dissolve 4-hydroxy-2-methylenepyrano[3,2-*c*]chromene-2,5-dione (1g) and gently refluxed for 4-5 hrs. After completion of the reaction, the mixture was poured onto crushed ice so the solid product of 3-acetyl-4-hydroxy-7-methyl-pyrano[3,2-*c*]chromene-2,5-dione was obtained. To obtain purity, product was dried and recrystallized from glacial acetic acid. The yield is found out to be about 71%.

***Synthesis of 4-hydroxy-7-methyl-3-(3-oxobutanoyl)pyrano [3,2-c]chromene-2,5-dione ($L^{IX}$)***

Acetyl derivatives, on its further reaction with ethyl acetate in presence of sodium, give acetoacetyl derivatives acetylation of different derivatives in presence of acetic acid and phosphorous oxychloride [9-14]. A solution of 3-acetyl-4-hydroxy-pyrano[3,2-c]chromene-2,5-dione (1.0 g) in ethyl acetate (25 mL) was added to pulverized sodium (1.0 g), and the reaction mixture was refluxed for 8 h. After completion of the reaction, the mixture was carefully decomposed with crushed ice and extracted with diethyl ether. The aqueous layer was acidified with dilute acid to afford substituted 4-hydroxy-7-methyl-3-(3-oxobutanoyl)pyrano[3,2-c]chromene-2,5-dione as a precipitate. The solid product was filtered, washed with water, dried, and recrystallized from acetone to obtain the purified compound. The yield is found out to be about 69%.

***Synthesis of metal complexes***

Metal(II) salt solutions (0.1 M) were prepared by dissolving ferrous ammonium sulphate and the chlorides of cobalt(II), nickel(II), and copper(II) in distilled water and were standardized using 0.1 M EDTA solution. The standardized metal solution (10 mL) was added slowly to the ligand solution (20 mL) with constant stirring. The reaction mixture was heated on a water bath at 100 °C for 2 h. The pH of the solution was maintained at 10.5–11.0 by the dropwise addition of ammonium hydroxide solution during the reaction. The resulting precipitates were filtered, thoroughly washed with distilled water followed by ethanol to remove unreacted materials, dried under vacuum, and recrystallized from dimethyl sulfoxide (DMSO) to afford the corresponding metal(II) complexes. The yield is found out to be about 65-71%.

Common structures of metal complexes are shown in **Figure 1** and overall reaction scheme is given in **Figure 2**.

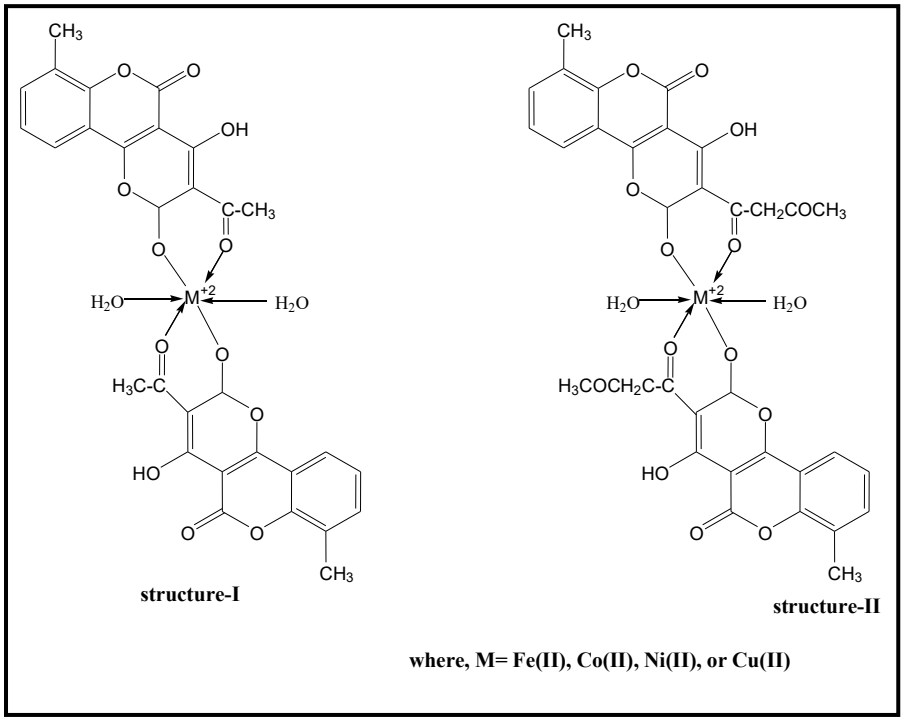


**Figure 1** Structure of metal complexes

***Antimicrobial activity***

*Quantitative antibacterial assay*

Different concentrations of the test compounds were evaluated for antimicrobial activity. The compounds were prepared at appropriate concentrations in a suitable growth medium and incubated with the test microorganisms under standard conditions. The lowest concentration of the compound that completely inhibited visible microbial growth was recorded as the minimum inhibitory concentration (MIC, mg $mL^{-1}$).

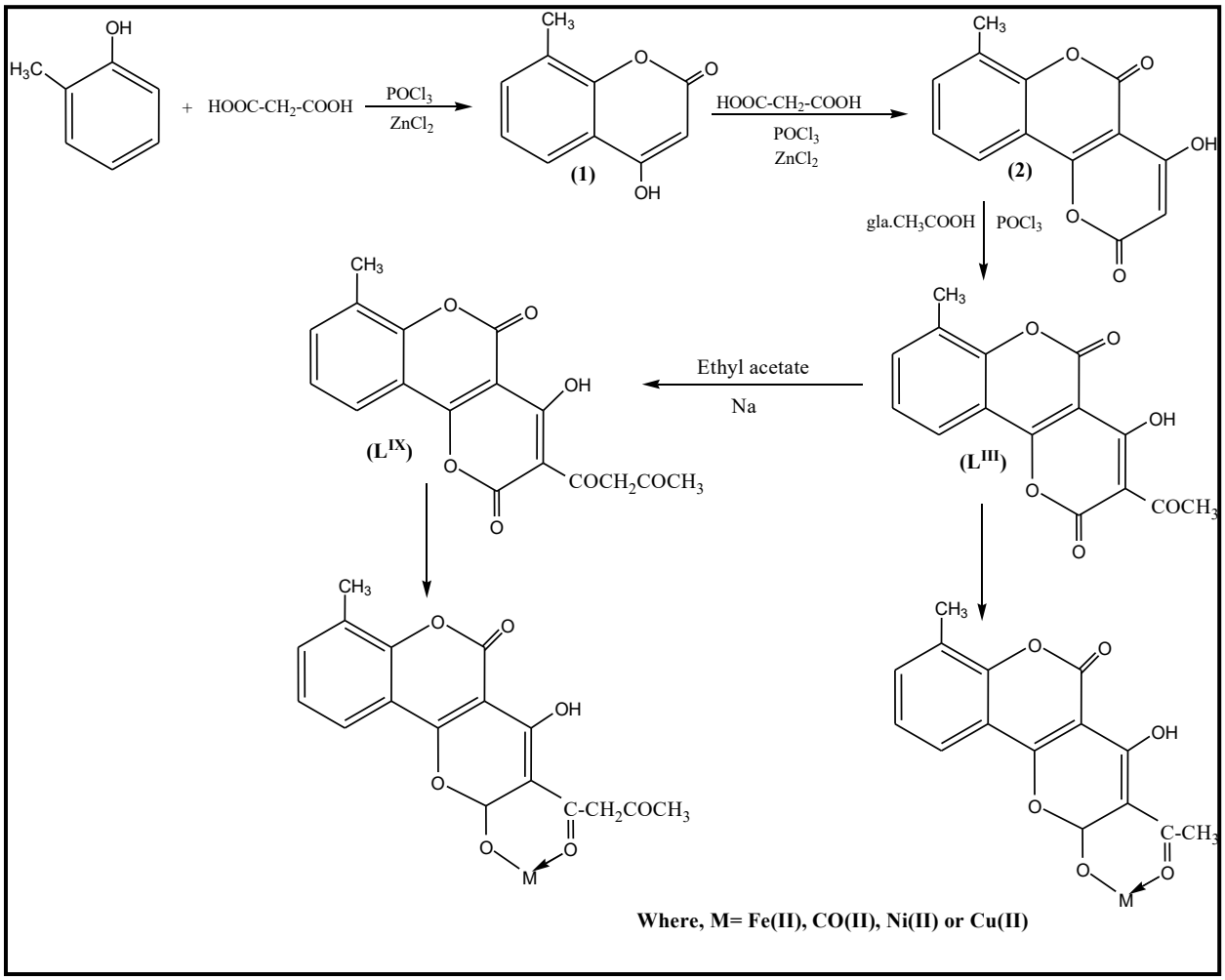


**Figure 2** Reaction scheme

*Qualitative antimicrobial assay*

The *in vitro* antimicrobial activity of the synthesized compounds was evaluated by the agar well diffusion (agar cup) method. Antibacterial screening was carried out against the Gram-negative bacterium *Escherichia coli* and the Gram-positive bacterium *Bacillus megaterium* using nutrient agar as the growth medium. Antifungal activity was assessed against *Aspergillus niger* and *Candida albicans* using glucose yeast extract (GYE) medium. Stock solutions of the test compounds were prepared in dimethyl sulfoxide (DMSO). Sterile agar plates were inoculated with the respective test microorganisms, and wells were made using a sterile borer. Aliquots of the test solutions at varying concentrations were carefully dispensed into the wells using a micropipette. The inoculated plates were incubated at 37 °C for 24 h in the case of bacterial strains and for 48 h for fungal strains. DMSO served as the control. Antimicrobial activity was determined by measuring the diameter of the clear zones of inhibition around the wells, expressed in millimeters (mm).

*Gel electrophoresis*

DNA cleavage activity of the metal complexes was evaluated by agarose gel electrophoresis using calf thymus DNA (CT-DNA) in the presence of $H_2O_2$ as an oxidizing agent. The reaction mixture consisted of CT-DNA (5 µL, $4 \times 10^{-4}$ µg µL$^{-1}$), test compound (12 µL, 1000 ppm), and $H_2O_2$ (2 µL, 35%). The mixtures were incubated at 35°C for 30 min prior to electrophoresis. The samples were subsequently subjected to electrophoresis on a 0.8% agarose gel using Tris–acetic acid–EDTA (TAE) buffer (pH 8.3) at a constant voltage of 50 V for 2 h. Following electrophoresis, the gel was stained with ethidium bromide (1 µg cm$^{-3}$) and visualized under UV illumination. Gel images were recorded using a Sony (India) camera.

## Result and Discussion

All the synthesized compounds were found to be stable at room temperature. They were insoluble in water, methanol, and ethanol but readily soluble in dimethylformamide (DMF) and dimethyl sulfoxide (DMSO). The analytical data

were consistent with the proposed stoichiometry and are summarized in **Tables 1** and **2**. Elemental analyses of the metal complexes indicated a metal-to-ligand (M:L) ratio of 1:2 for all divalent metal ions. As most of the metal complexes decomposed or charred above 270 °C, melting points could not be determined. The low molar conductance values of the complexes suggested their non-electrolytic nature [15].

**Table 1** Analytical and physical data of the synthesized compounds

| Sample | Substitution | | | | Molecular | Molecular | Melting | Rf | Colour |
|---|---|---|---|---|---|---|---|---|---|
| Code | $R_1$ | $R_2$ | $R_3$ | $R_4$ | Formula | Weight | Point ($^oC$) | Value | |
| 1 | H | H | H | $CH_3$ | $C_{10}H_8O_3$ | 176 | 208-210 | 0.69 | Ligth Orange |
| 2 | H | H | H | $CH_3$ | $C_{13}H_8O_5$ | 244 | 108-110 | 0.66 | Brown |
| $L^{III}$ | H | H | H | $CH_3$ | $C_{15}H_{10}O_6$ | 286 | 86-88 | 0.64 | Brown |
| $L^{IX}$ | H | H | H | $CH_3$ | $C_{17}H_{12}O_7$ | 328 | 102-104 | 0.61 | Dark Brown |

**Table 2** Physical characterization, analytical and molar conductance data of metal complexes

| Complex | Sample code | Molecular Formula | Molecular weight (g) | Elemental analysis(%) Found/Calcd. C | H | O | Molar conductance mho $cm^2mol^{-1}$ | Colour | Yield(%) |
|---|---|---|---|---|---|---|---|---|---|
| $Fe[L^{III}(H_2O)]_2$ | 336 | $C_{30}H_{26}O_{14}Fe$ | 666 | 54.25/54.07 | 3.9/3.93 | 33.51/33.61 | 10.59 | Dark Brown | 68 |
| $Co[L^{III}(H_2O)]_2$ | 337 | $C_{30}H_{26}O_{14}Co$ | 669 | 53.93/53.82 | 3.75/3.91 | 33.33/33.46 | 13.78 | Light Orange | 69 |
| $Ni[L^{III}(H_2O)]_2$ | 338 | $C_{30}H_{26}O_{14}Ni$ | 668 | 53.92/53.84 | 3.75/3.92 | 33.58/33.47 | 9.68 | Yellowish Brown | 65 |
| $Cu[L^{III}(H_2O)]_2$ | 339 | $C_{30}H_{26}O_{14}Cu$ | 673 | 53.56/53.45 | 4.02/3.89 | 33.09/33.23 | 12.93 | Brown | 70 |
| $Fe[L^{IX}(H_2O)]_2$ | 346 | $C_{34}H_{30}O_{16}Fe$ | 750 | 54.51/53.45 | 3.84/4.03 | 34.24/34.11 | 14.19 | Brown | 69 |
| $Co[L^{IX}(H_2O)]_2$ | 347 | $C_{34}H_{30}O_{16}Co$ | 753 | 54.21/54.19 | 3.93/4.01 | 34.01/33.97 | 10.54 | Reddish Brown | 66 |
| $Ni[L^{IX}(H_2O)]_2$ | 348 | $C_{34}H_{30}O_{16}Ni$ | 753 | 54.39/54.21 | 4.09/4.01 | 33.92/33.98 | 13.69 | Green | 67 |
| $Cu[L^{IX}(H_2O)]_2$ | 349 | $C_{34}H_{30}O_{16}Cu$ | 758 | 53.95/53.86 | 4.12/3.99 | 33.86/33.77 | 12.73 | Dark Brown | 71 |

### *Absorption Spectra*

Electronic spectroscopy was employed as an important tool for structural characterization of the synthesized compounds. UV spectra were recorded in the range 200–800 nm using DMSO as the solvent. The compounds exhibit absorption bands in the region 250–350 nm, attributed mainly to π→π* transition at 268 nm and n→π* transition at 338 nm. In general, absorption of UV–visible radiation by organic molecules involves electronic transitions such as σ→σ*, n→σ*, n→π*, and π→π*, corresponding to excitation of electrons from the ground state to higher energy antibonding orbitals; transitions involving unsaturated centres (n→π* and π→π*) typically occur at longer wavelengths.

The positions of the absorption bands for the synthesized derivatives were found to be nearly identical, indicating that substitution with acetyl or acetoacetyl groups did not significantly alter the position of band. Minor shifts in band positions were observed and may be attributed to differences in molecular weight. The electronic spectra of the metal complexes were recorded on a Shimadzu UV-1800 spectrophotometer using DMSO as solvent. The complexes displayed two prominent bands in the range 266–332 nm along with a weak band in the visible region at 741–749 nm.

### *IR Spectra (DMSO, $cm^{-1}$)*

**Ligands:** 3440 (OH) (enolic) [16], 1080 (C–O), 2932 (C-H), 1491–1550 (C=C), 667-730 (=C–H aromatic), 1723 (C=O cyclic), 1163–1294 (C–O–C), 1606–1612 (C=O α,β-unsaturated acetyl ketone), 1294–1330 (monodentate acetate coordination)

**Metal Complexes:** ~3440 (OH) (enolic almost unaffected), 2924 (C-H), 1448 (C=C), 848 (=C–H aromatic), 1681(C=O cyclic, coordination of carbonyl oxygen to metal), 1086-1253 (C–O–C), 1609-1612 (C=O α,β-unsaturated acetyl ketone), 476–486 (M–O vibrations, confirming metal–oxygen bonding) [17]

***$^1$H NMR Spectra (500 MHz, DMSO-d6)***

**Ligands:** δ 2.258–2.795 (s, $CH_3$), δ 6.527–7.616(m, Ar–H), δ 9.924 (s, –OH), δ 1.98 (s, –$COCH_3$), δ 4.1(s, –$COCH_2COCH_3$)
**Metal Complexes:** δ 2.357-2.550 (s, $CH_3$), δ 7.241-7.392 (m, Ar–H), δ 10.287 (s, –OH), δ 1.772(s, –$COCH_3$), δ 4.8 (s, $H_2O$)

***Mass Spectra***

The mass spectrum of compounds was recorded by GCMS-QP2010 spectrometer (EI method). The spectra were acquired in positive chemical ionization mass spectrometry. In each case, well-defined molecular ion ($M^+$) and base peaks were observed in the mass spectra. The observed molecular ion peak values were in good agreement with the calculated molecular weights, thereby confirming the proposed molecular formulae of the synthesized compounds.

**Table 3** Antimicrobial data of ligands & their metal complexes (Conc. in ppm & zone of inhibition in millimeter)

| Compound | *Escherichia coli* | | *Bacillus megaterium* | | *Aspergillus niger* | | *Candida albicans* | |
|---|---|---|---|---|---|---|---|---|
| | Conc.(ppm) | Zone(mm) | Conc.(ppm) | Zone(mm) | Conc.(ppm) | Zone(mm) | Conc.(ppm) | Zone(mm) |
| $L^{III}$ | 200 | 22 | 200 | 18 | 300 | 21 | 300 | 20.5 |
| | 300 | 23 | 300 | 19 | 400 | 21.5 | 400 | 21 |
| | 400 | 24.5 | 400 | 20.5 | 500 | 22 | 500 | 22 |
| $Fe[L^{III}(H_2O)]_2$ | 100 | 25 | 100 | 19.5 | 200 | 20 | 200 | 19 |
| | 200 | 26 | 200 | 20 | 300 | 21 | 300 | 21 |
| | 300 | 26.5 | 300 | 21.5 | 400 | 22 | 400 | 22 |
| $Co[L^{III}(H_2O)]_2$ | 100 | 24.5 | 50 | 18 | 200 | 21 | 200 | 20 |
| | 200 | 25 | 100 | 19.5 | 300 | 22 | 300 | 20.5 |
| | 300 | 25.5 | 200 | 21 | 400 | 23 | 400 | 22 |
| $Ni[L^{III}(H_2O)]_2$ | 100 | 23 | 100 | 20 | 300 | 22 | 300 | 21.5 |
| | 200 | 24 | 200 | 20.5 | 400 | 23.5 | 400 | 23 |
| | 300 | 25 | 300 | 22 | 500 | 24 | 500 | 23.5 |
| $Cu[L^{III}(H_2O)]_2$ | 100 | 23.5 | 100 | 19 | 200 | 22 | 200 | 20 |
| | 200 | 25 | 200 | 21 | 300 | 24 | 300 | 21 |
| | 300 | 26 | 300 | 21.5 | 400 | 25 | 400 | 23 |
| $L^{IX}$ | 200 | 25 | 200 | 18.5 | 300 | 22 | 300 | 22 |
| | 300 | 25 | 300 | 20 | 400 | 23 | 400 | 23.5 |
| | 400 | 25.5 | 400 | 21 | 500 | 23.5 | 500 | 24 |
| $Fe[L^{IX}(H_2O)]_2$ | 100 | 24.5 | 100 | 18 | 200 | 21 | 200 | 21 |
| | 200 | 25 | 200 | 19 | 300 | 22.5 | 300 | 22.5 |
| | 300 | 26 | 300 | 20.5 | 400 | 23 | 400 | 24 |
| $Co[L^{IX}(H_2O)]_2$ | 50 | 23 | 100 | 18.5 | 300 | 22 | 300 | 23 |
| | 100 | 25 | 200 | 20 | 400 | 24 | 400 | 23.5 |
| | 200 | 25.5 | 300 | 21 | 500 | 24.5 | 500 | 25 |
| $Ni[L^{IX}(H_2O)]_2$ | 100 | 25 | 50 | 18 | 200 | 21 | 200 | 22 |
| | 200 | 25 | 100 | 20 | 300 | 23 | 300 | 23 |
| | 300 | 25.5 | 200 | 21 | 400 | 23.5 | 400 | 24.5 |
| $Cu[L^{IX}(H_2O)]_2$ | 100 | 24 | 100 | 19 | 200 | 22 | 200 | 23 |
| | 200 | 26 | 200 | 20 | 300 | 23.5 | 300 | 25 |
| | 300 | 26 | 300 | 22 | 400 | 24.5 | 400 | 25 |

***Antimicrobial activity***

The antimicrobial activity of the ligand and its metal complexes was evaluated by determining the minimum inhibitory concentration (MIC) using the serial dilution method. The *in vitro* antimicrobial studies were carried out against *Escherichia coli*, *Bacillus megaterium*, *Aspergillus niger*, and *Candida albicans*. Based on the MIC results, the zones of inhibition were further measured (mm) using the disc diffusion method [18–21], and the data are summarized in

**Table 3**. Comparative evaluation **(Figure 3 and Figure 4)** indicated that the metal complexes exhibited enhanced antimicrobial activity compared with the free ligand.

The enhanced biological activity of the metal complexes can be rationalized on the basis of Overtone's concept of cell permeability and Tweedy's chelation theory. According to Overtone's concept, the lipid membrane surrounding microbial cells favours the passage of lipid-soluble substances; therefore, liposolubility plays an important role in antimicrobial efficiency. Upon chelation, the polarity of the metal ion is reduced due to partial sharing of the positive charge with donor atoms and overlap of ligand orbitals, leading to increased π-electron delocalization over the chelate ring. This enhanced lipophilicity facilitates penetration of the complexes through the lipid membrane and interaction with cellular targets, including metal-binding sites of enzymes. Consequently, the complexes may interfere with cellular respiration and protein synthesis, ultimately inhibiting the growth of the microorganisms.

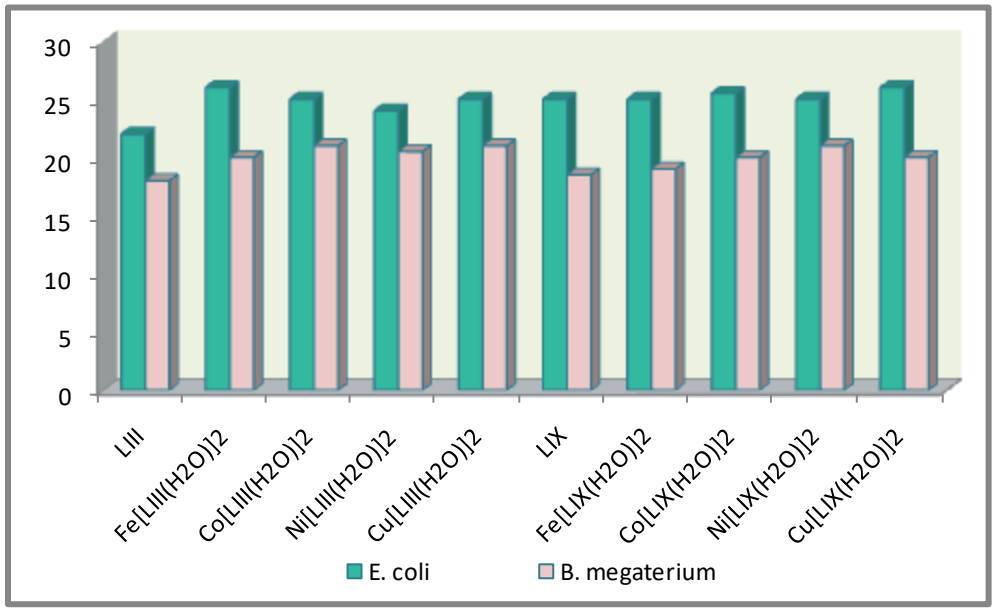


**Figure 3** Comparison of antibacterial data of the $L^{III}$, $L^{IX}$ and their metal complexes at 200ppm concentration

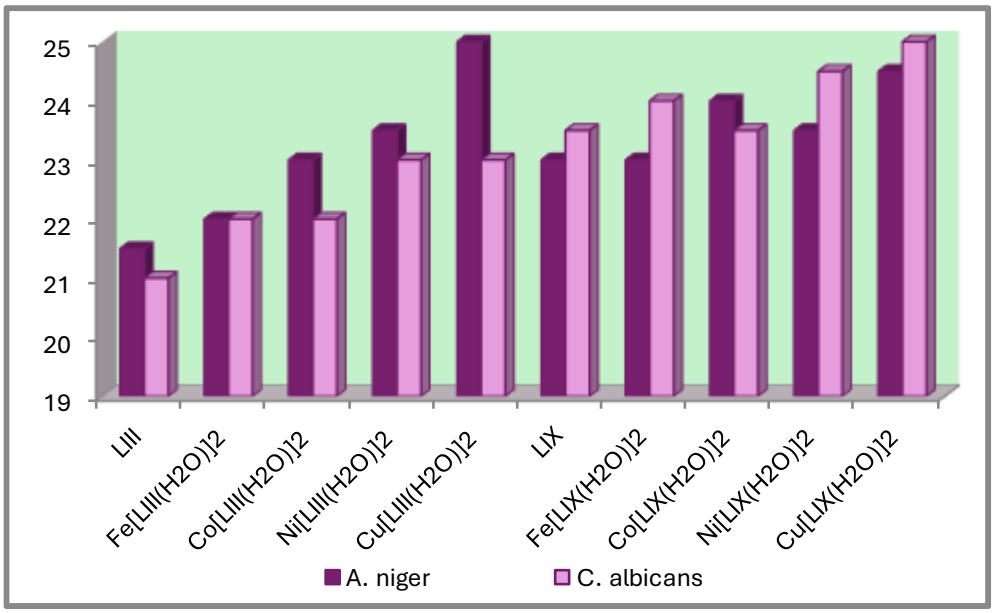


**Figure 4** Comparison of antifungal data of the $L^{III}$, $L^{IX}$ and their metal complexes at 400ppm concentration

***DNA Cleavage Studies***

The DNA cleavage efficiency of the complexes compared to the control can be attributed to their strong DNA-binding ability. The metal complexes were capable of inducing DNA degradation. The proposed oxidative mechanism involves DNA cleavage through hydroxyl radicals, which abstract hydrogen atoms from sugar moieties, leading to the release of specific sugar-derived fragments depending on the site of hydrogen abstraction [22]. The cleavage process is inhibited

in the presence of free radical scavengers, suggesting that hydroxyl radicals or peroxy species mediate the reaction. This process is facilitated by metallocomplex-bound hydroxyl radicals or peroxo species generated from the reaction with the co-reactant $H_2O_2$.

In the present study, CT-DNA gel electrophoresis experiments were performed at 35 °C using the synthesized complexes in the presence of $H_2O_2$ as an oxidizing agent. At very low concentrations, some complexes exhibited noticeable nuclease activity. In contrast, the control experiment using DNA alone showed no significant DNA cleavage even after prolonged exposure. This may be attributed to the redox behavior of the metal ions present in the complexes. The redox properties of the metal complexes facilitate the oxidation of nucleic acids. In the oxidative DNA cleavage mechanism, metal ions in the complexes react with $H_2O_2$ to generate hydroxyl radicals, which attack the C4 position of the sugar moiety, ultimately leading to DNA strand scission [23].

As a result of DNA cleavage, a decrease in the intensity of DNA bands was observed in the gel electrophoresis images **(Figures 5 and 6)**. A slight increase in complex concentration beyond the optimal level (the concentration at which 100% cleavage efficiency was observed) resulted in extensive DNA degradation, leading to the disappearance of DNA bands on the agarose gel [24-27].

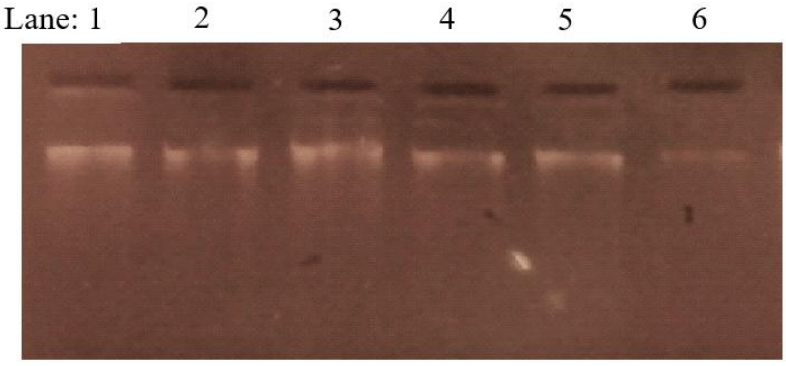


**Figure-5:** Agarose gel (0.8 %) showing the changes in the agarose gel electrophoretic pattern of CT DNA using ligand 3-acetyl-4-hydroxy-7-methylpyrano[3,2-*c*]chromene-2,5-dione **($L^{III}$)** and it's metal(II) complexes induced by $H_2O_2$. **Lane 1:** DNA alone, **Lane 2:** DNA + $L^{III}$, **Lane 3:** DNA + $Fe[L^{III}(H_2O)]_2$, **Lane 4:** DNA + $Co[L^{III}(H_2O)]_2$, **Lane 5:** DNA + $Ni[L^{III}(H_2O)]_2$, **Lane 6:** DNA + $Cu[L^{III}(H_2O)]_2$

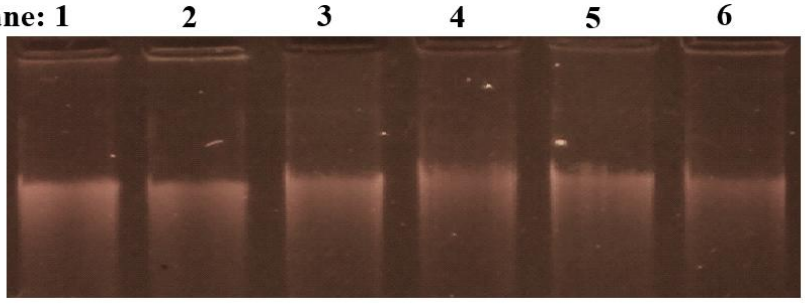


**Figure-6:** Agarose gel (0.8 %) showing the changes in the agarose gel electrophoretic pattern of CT DNA using ligand 3-acetyl-4-hydroxy-8-methylpyrano[3,2-*c*]chromene-2,5-dione**($L^{IV}$)** and it's metal(II) complexes induced by $H_2O_2$. **Lane 1:** DNA alone, **Lane 2:** DNA + $L^{IX}$, **Lane 3:** DNA + $Fe[L^{IX}(H_2O)]_2$, **Lane 4:** DNA + $Co[L^{IX}(H_2O)]_2$, **Lane 5:** DNA + $Ni[L^{IX}(H_2O)]_2$, **Lane 6:** DNA + $Cu[L^{IX}(H_2O)]_2$

## Conclusion

All metal complexes have lower conductance values (molar conductance <15 mho $cm^2mol^{-1}$; $10^{-3}$ M solution); that indicates complexes are non-electrolytes in DMF and metal is attached through coordinate covalent bond. All the spectral data of the synthesized complexes are in good agreement with the proposed structures (Structure 1 and 2). The antimicrobial activity data (Table 3) indicate that most of the metal complexes exhibit higher biological activity compared to their corresponding ligands. Figure 3 shows that all the synthesized compounds were active against both bacterial strains at a concentration of 200 ppm. Similarly, comparison of antifungal activity data at 400 ppm (Figure 4) demonstrates that all compounds exhibited significant activity against both fungal strains. $Fe[L^{III}(H_2O)]_2$ and $Cu[L^{IX}(H_2O)]_2$ against *E. coli* (zone of inhibition 26 mm), $Co[L^{III}(H_2O)]_2$, $Cu[L^{III}(H_2O)]_2$ and $Ni[L^{IX}(H_2O)]_2$ against *B. megaterium* (zone of inhibition 21 mm) at 200 ppm concentration while $Cu[L^{III}(H_2O)]_2$ against *A. niger* (zone of inhibition 25 mm), and $Cu[L^{IX}(H_2O)]_2$ against *C. albicans* (zone of inhibition 25 mm) shows higher activities. From

Figure 3 it can be concluded that $Cu[L^{III}(H_2O)]_2$ and from Figure 4 $Cu[L^{IX}(H_2O)]_2$ demonstrates minimun intensity band of DNA in the presence of $H_2O_2$, it leads to the conclusion that these complexes have highest DNA cleavage ability.

## References


[1] S. Akter, B.Y. Alhatlani, E.M. Abdallah, S. Saha, J. Ferdous, M.E. Hossain, F. Ali and S.M.A. Kawsar. Exploring Cinnamoyl-Substituted Mannopyranosides: Synthesis, Evaluation of Antimicrobial Properties, and Molecular Docking Studies Targeting H5N1 Influenza A Virus. Molecules. 2023;28:8001. https://doi.org/10.3390/molecules28248001

[2] T.J. Hossain, Methods for screening and evaluation of antimicrobial activity: A review of protocols, advantages, and limitations. European Journal of Microbiology and Immunology. 2024;14(2):97–115. https://doi.org/10.1556/1886.2024.00035

[3] G. Porras, F. Chassagne, J.T. Lyles, L. Marquez, M. Dettweiler, A.M. Salam, T. Samarakoon, S. Shabih, D.R. Farrokhi, C.L. Quave. Ethnobotany and the Role of Plant Natural Products in Antibiotic Drug Discovery. Chemical Reviews. 2021;121:3495–3560. https://dx.doi.org/10.1021/acs.chemrev.0c00922

[4] A.A. Rabaan, T. Sulaiman, S.H. Al-Ahmed, Z.A. Buhaliqah, A.A. Buhaliqah, B. AlYuosof, M. Alfaresi, M.A. Al Fares, S. Alwarthan, M.S. Alkathlan et al. Potential Strategies to Control the Risk of Antifungal Resistance in Humans: A Comprehensive Review. Antibiotics. 2023;12:608. https://doi.org/10.3390/antibiotics12030608

[5] R.K. Sodhi, S. Paul. Metal Complexes in Medicine: An Overview and Update from Drug Design Perspective. Cancer Therapy & Oncology International Journal. 2019;14(2):555883. DOI:10.19080/CTOIJ.2019.14.555883

[6] C. Orvig, M.J. Abrams. Medicinal inorganic chemistry: introduction. Chemical Reviews. 1999;99(9):2201–2204. DOI: 10.1021/cr980419w

[7] J. Marmur. A Procedure For The Isolation of Deoxyribonucleic Acid For Micro-Organisms. Journal of Molecular Biology. 196;3:208–218. https://doi.org/10.1016/S0022-2836(61)80047-8

[8] N. Bhatt, A. Shah, R.V. Raval, V.M. Thakor. NOVEL SYNTHESIS OF BENZOFURANS. Current Social Sciences. 1984:53:1289–1290.

[9] R. Anschutz. Europian Journal of Organic Chemistry. 1909; 867:169. https://doi.org/10.1002/jlac.19093670108

[10] V.N. Dholakia, M.G. Parekh, K.N. Trivedi. Studies in 4-hydroxy coumarins. II. α- and γ- Pyrones from 4-hydroxy coumarins. Australian Journal of Chemistry. 1968;21(9):2345–2347. https://doi.org/10.1071/CH9682345

[11] H.R. Eisenhaur, K.P. Link. Studies on 4-Hydroxy- Coumarins. XIII. The Mechanism for the Reaction of 4-Hydroxycoumarin with Aliphatic Acid Chlorides. Journal of American Chemical Society. 1953;75:2044. https://doi.org/10.1021/ja01105a006

[12] H. Pauly, K. Lockmann. Formation of monophenol ketones and a new synthesis on benzotetronic acid. Europian Journal of Inorganic Chemistry. 1915;48:28-32. https://doi.org/10.1002/cber.19150480107

[13] A. Sonn. About β-oxycoumarins. Reports of the German Chemical Society. 1917;50:1292. https://doi.org/10.1002/cber.19170500229

[14] M.A. Stahmenn, I. Wolff, K.P. Link. Journal of American Chemical Society.1943; 65:2285. https://doi.org/10.1021/ja01252a007

[15] W.J. Geary. The use of conductivity measurements in organic solvents for the characterisation of coordination compounds. Coordination Chemistry Reviews.1970;7:81–122. https://doi.org/10.1016/S0010-8545(00)80009-0

[16] L.J. Bellamy. The Infrared Spectra of Complex Molecules, Chapman and Hall, London, 1980.

[17] K. Nakamoto. Infrared Spectra and Raman Spectra of Inorganic and Coordination Compounds, John Wiley and Sons, New York, 1997.

[18] N. Dharmaraj, P. Viswanathamurthi, K. Natarajan. Ruthenium(II) complexes containing bidentate Schiff bases and their antifungal activity. Transition Metal Chemistry. 2001;26:105. https://doi.org/10.1023/A:1007132408648

[19] M.J. Pelczar, E.C.S. Chan, N.R. Krieg. Microbiology, Blackwell Science, New York, 1998.

[20] E.J. Stokes, G.L. Ridgway. Clinical Bacteriology, Edward Arnold Publisher, Maryland, USA, 1980.

[21] C.H. Colins, P.M. Lyne. Microbial Methods, Univ. Park Press, Baltimore(Maryland, USA), 1970.

[22] Prativel G, Pitie M, Bernadou J, Meunier B. Furfural as a marker of DNA cleavage by hydroxylation at the 5′ carbon of deoxyribose. Angewandte Chemie International Edition. 1991;30:702. https://doi.org/10.1002/anie.199107021

[23] N. Raman, L. Mitu, A. Sakthivel, M.S.S. Pandi. Studies on DNA cleavage and antimicrobial screening of transition metal complexes of 4-aminoantipyrine derivatives of N2O2 type. Joural of Iranian Chemical Society. 2009;6(4):738–748. https://doi.org/10.1007/BF03246164

[24] R.R. Joshi, K.N. Ganesh. Metallodesferals as a new class of DNA cleavers: Specificity, mechanism and targetting of DNA scission reactions. Journal of Chemical Sciences. 1994;16:1089. https://doi.org/10.1007/BF02841918

[25] R Neelaveni, S Vasantha, R Keerthana, S Sivakolunthu, T Angeline. DNA cleavage activity of novel schiff base copper(II) complexes with sulfur containing-ligands: (2-(2-methylthio)phenylimino)methylphenol, N-benzylidine-2-methylthioaniline. Asian Journal of Pharmacuitical and Clinical Research. 2016;9(3):277-281

[26] S. Harishkumar,N.D. Satyanarayan. DNA cleavage potential of 4-(piperidin-1- ylmethyl)-2-(thiophen-2-yl) quinoline analogues. Indo American Journal of Pharmaceutical Sciences. 2018;05(03):2023-2026.

[27] Z. Rozmer, A. Bernardes, C.N. Pérez, P. Perjési. Study on the Interaction of 4'-Hydroxychalcones and their Mannich Derivatives with Calf Thymus DNA by TLC and Spectroscopic Methods, a DNA Cleavage Study. The Open Medicinal Chemistry Journal. 2020;14:122-131. DOI: 10.2174/1874104502014010122.



Publication History

| | |
|---|---|
| Received | 13.03.2026 |
| Revised | 21.03.2026 |
| Accepted | 22.03.2026 |
| Online | 30.04.2026 |